



NRC Publications Archive Archives des publications du CNRC

Tools for experimental characterization of the non-uniform rotational distortion in intravascular OCT probes

Dufour, Marc L.; Bisailon, Charles Étienne; Lamouche, Guy; Vergnole, Sébastien; Hewko, Mark; D'Amours, Frédéric; Padioleau, Christian; Sowa, Michael

This publication could be one of several versions: author's original, accepted manuscript or the publisher's version. /
La version de cette publication peut être l'une des suivantes : la version prépublication de l'auteur, la version acceptée du manuscrit ou la version de l'éditeur.

Publisher's version / Version de l'éditeur:

Proceedings of SPIE, 7883, 2011

NRC Publications Record / Notice d'Archives des publications de CNRC:

<https://nrc-publications.canada.ca/eng/view/object/?id=7b151ef0-f339-4849-87d8-2c3e10ce6502>
<https://publications-cnrc.canada.ca/fra/voir/objet/?id=7b151ef0-f339-4849-87d8-2c3e10ce6502>

Access and use of this website and the material on it are subject to the Terms and Conditions set forth at

<https://nrc-publications.canada.ca/eng/copyright>

READ THESE TERMS AND CONDITIONS CAREFULLY BEFORE USING THIS WEBSITE.

L'accès à ce site Web et l'utilisation de son contenu sont assujettis aux conditions présentées dans le site

<https://publications-cnrc.canada.ca/fra/droits>

LISEZ CES CONDITIONS ATTENTIVEMENT AVANT D'UTILISER CE SITE WEB.

Questions? Contact the NRC Publications Archive team at

PublicationsArchive-ArchivesPublications@nrc-cnrc.gc.ca. If you wish to email the authors directly, please see the first page of the publication for their contact information.

Vous avez des questions? Nous pouvons vous aider. Pour communiquer directement avec un auteur, consultez la première page de la revue dans laquelle son article a été publié afin de trouver ses coordonnées. Si vous n'arrivez pas à les repérer, communiquez avec nous à PublicationsArchive-ArchivesPublications@nrc-cnrc.gc.ca.



Tools for experimental characterization of the non-uniform rotational distortion in intravascular OCT probes

Marc L. Dufour^{*a}, Charles-Etienne Bisaillon^a, Guy Lamouche^a, Sebastien Vergnole^a, Mark Hewko^b, Frédéric D'Amours^a, Christian Padioleau^a, Michael Sowa^b

^aIndustrial Material Institute (IMI), National Research Council Canada (NRCC), 75 de Mortagne, Boucherville, Canada, J4B-6Y4; ^bInstitute for Biodiagnostic (IBD), NRCC,

*marc.dufour@cnrc-nrc.gc.ca

ABSTRACT

The Industrial Material Institute (IMI) together with the Institute for Biodiagnostic (IBD) has developed its own optical catheters for cardiovascular imaging applications. Those catheters have been used experimentally in the in vitro coronary artery model of the Langendorff beating heart and in a percutaneous coronary intervention procedure in a porcine model. For some catheter designs, non-uniform rotational distortion (NURD) can be observed as expected from past experience with intra-vascular ultrasound (IVUS) catheters.

A two-dimensional (2D) coronary artery test bench that simulates the path that gives access to the coronary arteries has been developed. The presence or absence of NURD can be assessed in the test bench using custom-built cardiovascular Optical Coherence Tomography (OCT) imaging system. A square geometry instead of the circular shape of an artery is used to simulate the coronary arteries. Thereby, it is easier to visualize NURD when it is present. The cumulated torsion induced by the friction on the catheter is measured along the artery path.

NURD is induced by the cumulated torsion force that is balanced by the varying friction force. Thus pullback force was measured and is correlated with NURD observed in the 2D test bench. Finally, a model is presented to help understanding the mechanical constraint that leads to the friction force variations.

Keywords: OCT, catheterized probes, NURD, pullback force, coronary artery

1. INTRODUCTION

The first demonstration of OCT as a tool for intravascular imaging was performed in a rabbit aorta and reported in an article published in 1999 [1]. Since then, OCT technology has evolved tremendously in speed and image quality especially with the introduction of Fourier domain optical coherence tomography [2]. However, the optical catheters in use today are still more-or-less based on the same basic optical design which includes a grin lens followed by a right angle prism at the distal end of a single-mode optical fiber. Continuous rotation and a pullback are used for cylindrical mapping of the internal structure of an artery.

The optical catheter, nearly two meters in length, rotates within a transparent polymer sheath typically introduced into the vasculature from the femoral artery. The access to the coronary arteries passes by several curved paths such as the aorta and the tight passage from the aorta to the coronary artery. The coronary arteries may also be tortuous. Inevitably, friction occurs along the catheter. The cumulated torsion force balanced by the varying friction force induces non uniform rotation distortion (NURD) already known from experience with intra-vascular ultrasound (IVUS) catheters [3] [4]. NURD is probably inevitable but keeping it within acceptable limits is possible and is a real design challenge.

The optical catheter focusing optics may be designed to have the same diameter as the single-mode optical fiber with its basic protective coating of less than 250 μm .

IMI together with IBD has developed its own optical catheters for cardiovascular applications, such as the monitoring of stent deployment. Some tools developed for evaluating the mechanical performance of these catheters are presented here.

2. OPTICAL DESIGN

2.1 Imaging strategy

The optical imaging approach used for OCT intravascular imaging is very similar to the one already in use for Intravascular Ultra-Sound (IVUS). An optical probe at the end of an optical fiber, called the optical catheter, is put in rotation inside a static transparent sheath. The probe beam is projected in a perpendicular direction to the rotation axis with the help of a right angle prism, towards the inside surface of the artery. A complete section of the artery is imaged by pulling back the catheter over the desired length and provides a cylindrical mapping of the surface. The optical catheter, the sheath and the compliant balloon have been developed at IMI for OCT imaging of coronary arteries. They are illustrated in Figure 1. The outside diameter (O.D.) of the optical catheter is 0.7 mm and the inside diameter (I.D.) of the sheath is 1.0 mm. The system has been used in porcine heart ex-vivo as illustrated in Figure 2, and in-vivo.

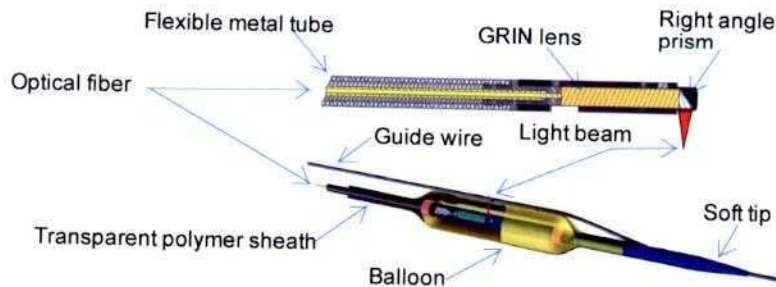


Figure 1. Optical catheter (top). Optical catheter inside the sheath (bottom). The optical catheter rotates inside the sheath.

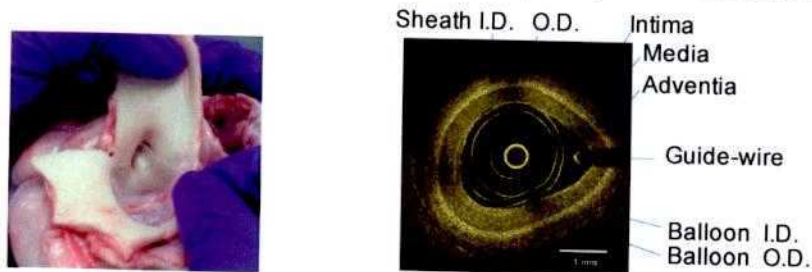


Figure 2. Introduction of the catheter inside a coronary artery of a porcine heart obtained from a slaughterhouse (left) and OCT image obtained of a porcine coronary artery using IMI's intravascular imaging system (right). I.D. stands for inside diameter and O.D. stands for outside diameter.

It has also been used for imaging coronary arteries in an isolated porcine beating heart. The laboratory setup for the isolated porcine beating heart was similar to the one previously used for understanding cardiac tissue oxygenation as a function of blood flow using near-infrared spectroscopy [5].

2.2 Imaging requirements

The coronary arteries have a tapered shape with an internal diameter of 3 to 4 mm in diameter, proximal to aorta. Their length is in the range of 10 cm. The external diameter of the sheath will eventually limit the distance along the coronary that the OCT imaging probe will be able to reach. The ability of the optical catheter to rotate smoothly while being pulled back into short radius bended path will eventually limit the usability of the OCT imaging system into side-branches. Therefore, the external diameter of the sheath should be smaller than 1.5 mm. The optical catheter should be able to move freely inside the sheath. Its external diameter should then have an external diameter lower than about 0.8 mm.

Blood is opaque to light and must be temporarily displaced. A first option is to use a compliant balloon. Practical lengths for a balloon are in the range of 5 mm to 40 mm. Occlusion time can be up to around 30-40 s [6] [7] but it would be better to target a shorter time. The balloon on top of a sheath makes the assembly less flexible than the sheath alone and more difficult to move into position.

Another option consists in flushing the artery with a transparent saline solution, without occlusion. Practical time limit is of around 4-5 s because of the volume of saline solution that must be injected. For the same reason, the number of

repetition must also be controlled during a given period of time. That flushing technique typically requires faster optical scan rate and pullback speed. Yet another option is called flush with occlusion [8] which is an alternative that requires a smaller amount of saline solution for flushing.

3. NON UNIFORM ROTATION DISTORTION (NURD)

3.1 NURD in coronary arteries

The mechanical drive provides a very stable rotation speed at the proximal end. The probe tip at the distal end rotates at the same averaged rotation speed but with some instability. The balance between the optical catheter shaft torsion stiffness against the cumulated friction against the sheath is responsible for that instability. This behavior is well documented [3] from past experience with rotating IVUS catheters that have a similar geometry. Friction must be balanced by an equivalent torque from the motor drive. The limited shaft torsion stiffness induced a cumulated torsion delay between the drive and the tip. Any friction variation implies an equivalent motor torque adjustment and implies a proportional cumulated torsion angular delay variation.

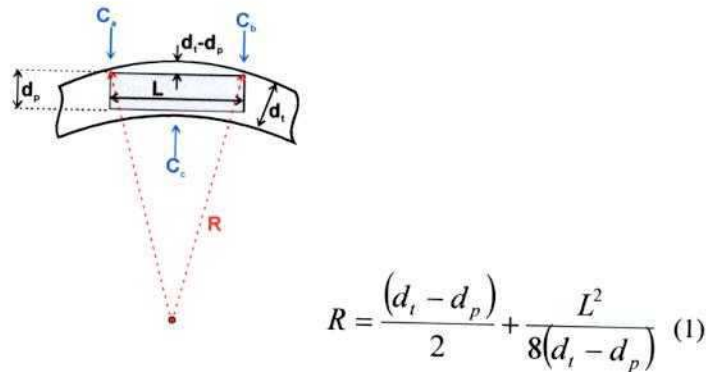
The model in Figure 3 (right) simulates the catheter behavior observed in Figure 3 (left). The model is used to remap the A-scans obtained in cylindrical coordinates from the catheter probe into a Cartesian coordinates image. The model replaces the uniform rotation speed assumption by a map of varying rotation speed while keeping the average speed constant over one full rotation. In this example, the catheter rotates at the same constant speed (relative speed 1x) most of the time. When the friction increases, the speed is reduced to 25% of the normal speed (relative speed 0.25x), thereby increasing the cumulated torsion in the catheter shaft. When the friction comes back to its normal value, the higher torque in the shaft (higher cumulated torsion) induces a speed increase (relative speed 3x) until the normal torque-friction equilibrium is reached.



Figure 3. NURD observed while imaging a coronary artery (left) within a beating heart (middle) and image created using a mathematical model that simulates rotation speed variations (right).

3.2 Probe geometrical considerations

Friction at the probe tip results from the contact of the probe with the sheath in tortuous paths. As illustrated in the model illustrated in Figure 4. The tip from the optical catheter comes in contact with the sheath on 3 points: the corner at each end C_a , C_b and the center C_c .



$$R = \frac{(d_t - d_p)}{2} + \frac{L^2}{8(d_t - d_p)} \quad (1)$$

Figure 4. Geometrical model of the probe tip in contact with the sheath.

The bending radius of the sheath at which the 3 points make contact is determined by the rigid length of the probe tip and the difference between the inside diameter of the sheath, d_s , and the diameter of the probe, d_p . R is the radius of curvature measured at the center of the sheath. Friction between the probe and the sheath may be tolerated as long as it is constant over a full turn. The probe circular symmetry at those contact points is thus very important.

4. NURD 2D TEST BENCH

4.1 Nurd test bench

Low-resolution images (<http://www.bmb.leeds.ac.uk/illingworth/visible/vismale.htm#current>) from the Visible Human Dataset (http://www.nlm.nih.gov/research/visible/visible_human.html) supplied by the US National Library of Medicine were used to retrace the three dimensional path that must be followed to access the coronary arteries of a human body through the aorta. With the help of image segmentation algorithm the 3D map of subset of the coronary arteries was obtained. The 3D map was converted to a 2D map by tilting the paths while preserving the radius of curvature of the paths. For the purpose of NURD testing, the 3D curvature may be projected in a single plane as long as the radius of curvature is preserved. The 2D map was then used to groove channels, 1.4 mm deep in a polymer material plate as illustrated in Figure 5.

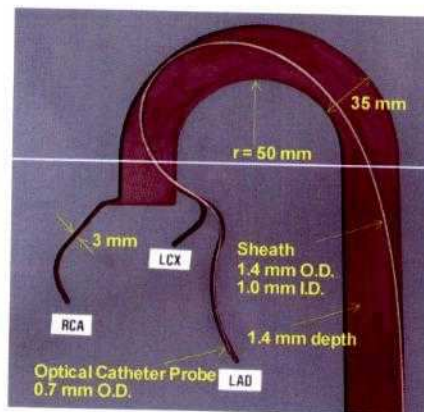


Figure 5. Coronary artery 2D model developed at IMI for NURD testing. The aorta, the right coronary artery (RCA), the left anterior descending artery (LAD) and the left circumflex artery (LCx) are grooved in the plate.

4.2 Observation of NURD in the test bench using OCT cardiovascular imaging system

The sheath was manually installed along the grooved paths of the test bench. As it is illustrated in Figure 6, the distal extremity of the sheath was placed at the end of the LAD branch. The sheath was held in place with the help of acrylic polymer sheets (not shown) simply deposited on the top surface of the test bench. The optical catheter was then inserted inside the sheath up to the distal extremity of the sheath.

The optical catheter was rotated at the rate of 4 turns/s, thereby providing cross-sectional images of the rectangular channels grooved in the test bench. OCT images were then continuously recorded while pulling back the optical catheter at the rate of 2 mm/s for 11 cm. Selected images recorded during the pullback are illustrated in Figure 6.

Mild NURD may be observed in the first image at 0 mm while the optical catheter is at the distal extremity of the LAD branch. NURD is practically non-existent when the optical catheter moves out of the LAD branch as seen of the last OCT image at 105 mm. However, when the probe tip of the optical catheter passes through the smaller radius curve around 75mm, strong NURD is observed.

An attempt to evaluate the torque induced by friction may start by measuring the variation of the cumulated torsion of the optical catheter at the probe tip. The angular position of each of the four corner of the rectangular shape of the simulated artery branch may be identified on the OCT images during the pullback. By computing the average of those values, the graphic in Figure 7 was obtained. An angular variation peak is observed at a distance of 75 mm which corresponds to the passage of the probe tip in the smallest radius curve.

A torsion peak is also observed when the link with the flexible metal tube, located 40 mm before the probe tip, passes through the same curve. The probe tip is located at 35 mm from the beginning when that occurs. The link is rigid over several millimeters because of the glue and induces more friction in small radius curves.

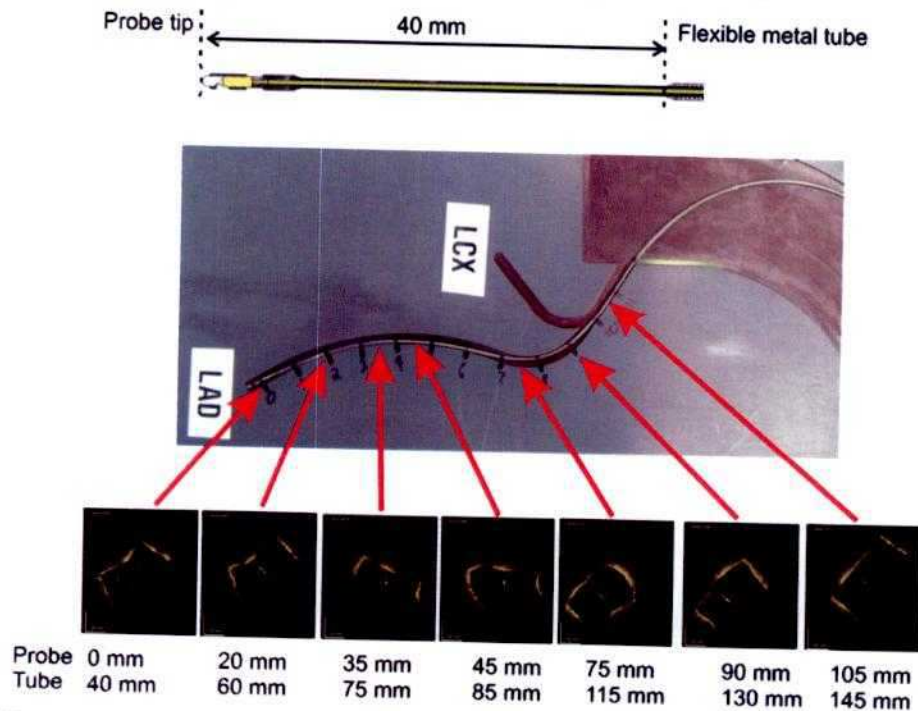


Figure 6. NURD observed using the OCT intravascular imaging catheter inside the 2D coronary artery model, both developed by IMI and IBD. The optical catheter (top) was rotating at the rate of 4 turns/s inside the sheath and pulled back from the extremity of the LAD branch (middle) along 11 cm at a speed of 2 mm/s OCT images at several locations during the pullback are illustrated (bottom).

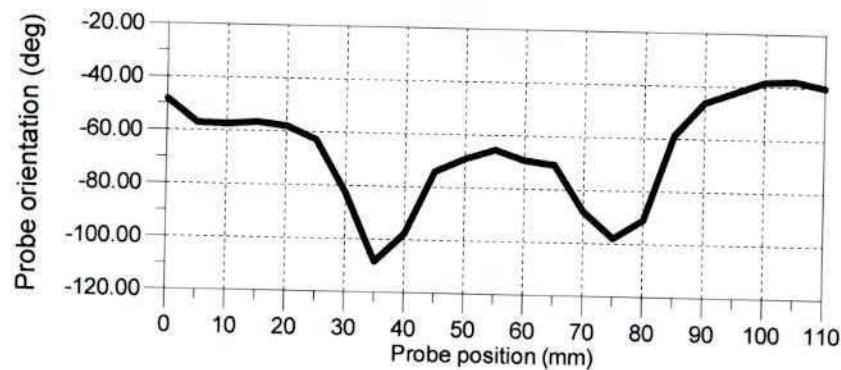


Figure 7. Optical probe orientation estimated during a pullback in the test bench

4.3 Recovering undistorted image

The data used to obtain images during a pullback are acquired in cylindrical coordinates. One A-scan corresponds to one particular orientation of the catheter and the position along one A-scans corresponds to the radius. A number of A-scans are accumulated while the catheter is making one full turn. A Cartesian image is obtained by remapping each point of each A-scans to their corresponding Cartesian coordinates. In that process, it is assumed that the A-scans are evenly distributed along one turn or that the rotation speed is uniform. In practice, the rotation speed is often varying during a single turn thereby inducing image distortions.

When imaging our test bench channels, we know exactly what the resulting image should be if there was no NURD. It is now our intention to compare the images obtained on the premise of a uniform rotation speed with the real shape of the channels. We intend to obtain a map of the real angular position of each A-scan made during one turn. Using that information, it will become possible to compute the instantaneous rotation speed along one turn and thereby to quantify the NURD.

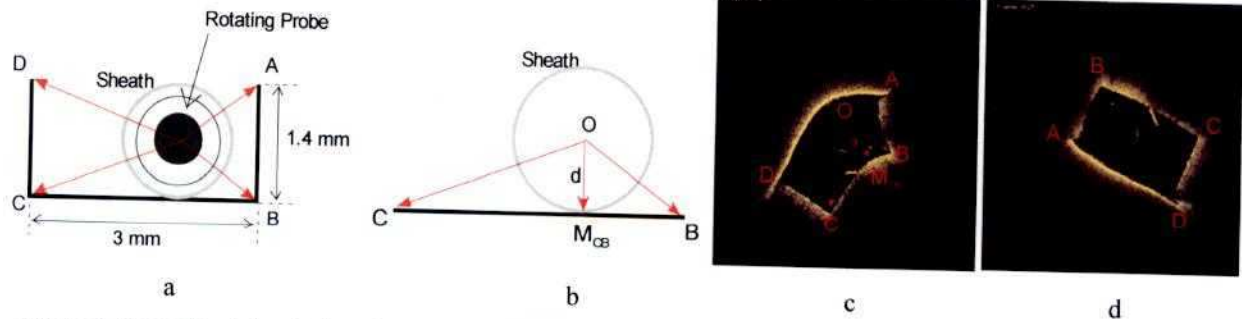


Figure 8. Geometrical description of a test bench channel (a), geometrical model of the bottom surface of a channel (b), a typical distorted image (c) and the undistorted image obtained by using the corrected angular map of the A-scans (d).

The shape of the channels grooved in the test bench is described in Figure 8a. The bottom segment C-B is detailed in Figure 8b and highlighted in a typical distorted image illustrated in Figure 8c. The curved line segment C-M_{CB}-B in the distorted image of Figure 8c corresponds to the straight line C-M_{CB}-B in the model in Figure 8b. Our first step in the process of recovering the correct angular mapping of the A-scans included in that image portion consists in finding the distance O-M_{CB}. One approach would be to use an image segmentation technique to identify the curved line C-B in Figure 8c and then to obtain a mathematical equation using a curve fitting technique. The rotation axis of the probe is, by definition, the center of the image. One can easily find the distance O-M_{CB} by comparing the curve-fitted equation with the location of the rotation axis.

It can be demonstrated that the distance of each point of the bottom surface relative to the probe rotation axis is unique for each A-scan within the line segment C-M_{CB}. The distortion in the image in Figure 8c is the result of a wrong angular mapping of the A-scans involved for that image portion. For each of those A-scans, one can find the distance of the bottom surface in Figure 8c, and then, find the point in Figure 8b that corresponds to the same distance. The correct angular position of that point is then computed using the model of Figure 8b (a triangle) and its value is used to update the angular mapping of the corresponding A-scans in Figure 8c. By pursuing that process for each line segment that defines the surface of the channel, one can compute the correct angular map for the full frame and obtain an undistorted image as the one displayed in Figure 8d. The reference point C in the undistorted image was arbitrarily defined as the beginning of the frame (angular position equals zero).

4.4 Pullback force measurement

The force required for inserting or removing an optical catheter inside or from a sheath may be measured using a setup such as the one illustrated in Figure 9. The measurement was made with an Instron Micro Tester 5548.

In this experiment, the hypothesis to be verified was that the pullback force measurement may be used as a mean to anticipate the rotational friction and resulting NURD amplitude along the artery during a pullback.

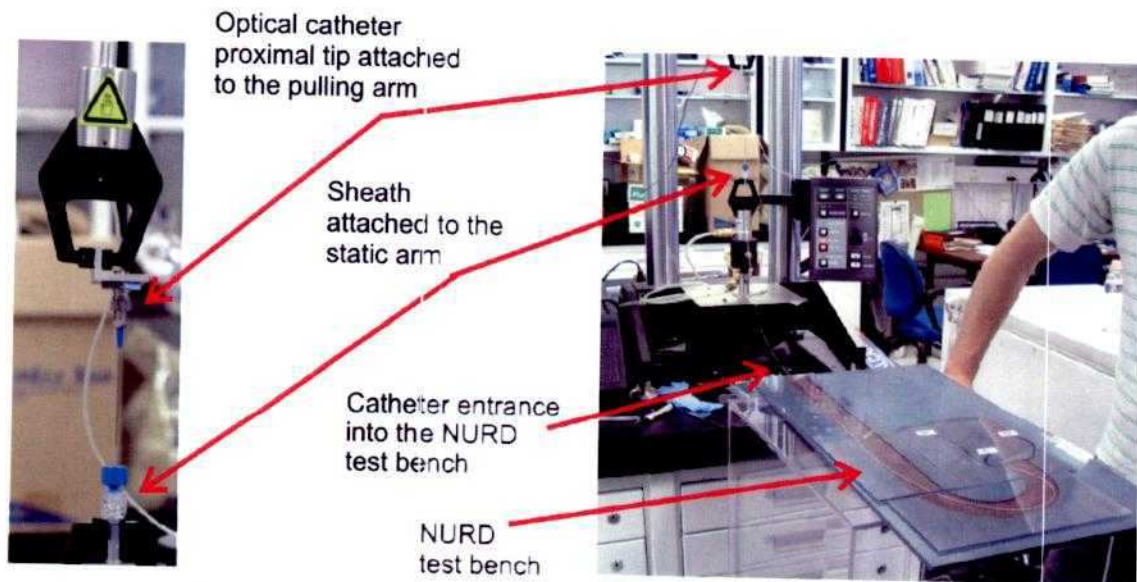


Figure 9. Setup for measuring the force required for pulling back the optical catheter located inside a sheath from a distal location to a proximal location.

A dummy probe having a similar geometrical shape as the imaging probe previously described was used. The length of the optical catheter, between the probe tip and the metallic tube, was shorter: 30 mm instead of 40 mm.

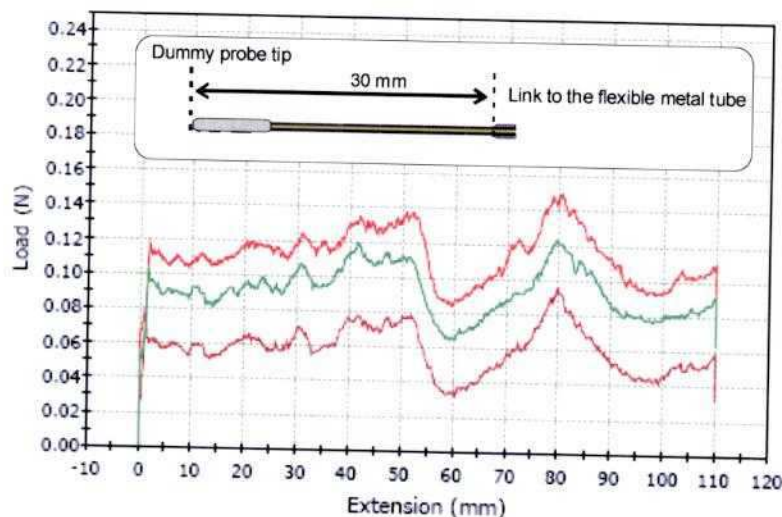


Figure 10. Force measured while pulling back the dummy optical catheter located inside the LAD branch of the 2D coronary artery model. The three curves in the graph are the signature of three pullback made under the same conditions. The force offset at the origin is induced by static friction.

The pullback force signature is similar to the torsion variation observed by the optical probe measured from OCT images. Two peaks are observed one at 80 mm when the probe tip passes through the small radius curve and the other peak is visible at 50 mm when the link to the flexible metal tube passes to through the same curve. There is a small location difference for the peak that corresponds to the passage of the link because it was closer to the tip in this particular experiment.

5. CONCLUSIONS

In this paper we have demonstrated that the geometrical context of the heart that is responsible for NURD can be simulated using a simple 2D test bench. Moderate NURD can be simulated with a simple mathematical model and quantified. The signature of pullback force measurements may be used to anticipate NURD for a given probe geometry even if the optical elements are not fully integrated.

6. REFERENCES

- [1] Fujimoto, J.G., et al., "High resolution in vivo intra-arterial imaging with optical coherence tomography", *Heart British Cardiac Society*, 82(2), 128-33 (1999).
- [2] Tearney, G.J., I.-K. Jang, and B.E. Bouma, "Optical coherence tomography for imaging the vulnerable plaque", *Journal of Biomedical Optics*, 11(2), 021002-10 (2006).
- [3] Kawase, Y., et al., "Comparison of nonuniform rotational distortion between mechanical IVUS and OCT using a phantom mode", *Ultrasound in Medicine and Biology*, 33(1), 67-73 (2007).
- [4] Vogt M, et al., "Estimation of 2D displacement and strain field in high frequency ultrasound based elastography", 2004 IEEE Ultrasonics Symposium IEEE Cat. No.04CH37553 2004: 376 9 Vol.1, (2005).
- [5] Nighswander-Rempel, S.P., V.V. Kupriyanov, and R.A. Shaw, "Regional cardiac tissue oxygenation as a function of blood flow and pO₂: a near-infrared spectroscopic imaging study", *Journal of Biomedical Optics*, 11(5). 054004-1 054004-10 (2006).
- [6] Kawase, Y., et al., "In vivo volumetric analysis of coronary stent using optical coherence tomography with a novel balloon occlusion-flushing catheter: A comparison with intravascular ultrasound", *Ultrasound in Medicine and Biology*, 31(10), 1343-1349 (2005).
- [7] Yamaguchi, T., et al., "Safety and Feasibility of an Intravascular Optical Coherence Tomography Image Wire System in the Clinical Setting", *The American Journal of Cardiology*, 101(5), 562-567 (2008).
- [8] Asawa, K., et al., "Method analysis for optimal continuous imaging using intravascular optical coherence tomograph", *J Cardiol*, 47(3), 133-41 (2006).